Available online at www.sciencedirect.com

ScienceDirect

journal homepage: www.jfda-online.com

Original Article

Biotransformation of mogrosides from *Siraitia grosvenorii* by *Ganoderma lucidum* mycelium and the purification of mogroside III E by macroporous resins

Chun-Hui Chiu [a,b,1], *Reuben Wang* [c,1], *Shasha Zhuang* [d], *Pei-Yin Lin* [e], *Yi-Chen Lo* [d,**], *Ting-Jang Lu* [d,*]

[a] *Institute of Health Industry and Technology, Research Center for Food and Cosmetic Safety, College of Human Ecology, Chang Gung University of Science and Technology, Taoyuan, Taiwan*
[b] *Department of Traditional Chinese Medicine, Chang Gung Memorial Hospital, Keelung, Taiwan*
[c] *Department of Food Science, Tunghai University, No. 1727, Sec. 4 Taiwan Boulevard, Xitun District, Taichung, Taiwan*
[d] *Institute of Food Science and Technology, National Taiwan University, Taipei, Taiwan*
[e] *Joint Center for Instruments and Researches, College of Bioresources and Agriculture, National Taiwan University, Taipei, Taiwan*

ARTICLE INFO

Article history:
Received 2 December 2018
Received in revised form
8 May 2019
Accepted 10 May 2019
Available online 29 May 2019

Keywords:
Biotransformation
Diaion® HP-20
Ganoderma lucidum
Mogroside III E
Sweetener

ABSTRACT

Mogrosides are the major triterpenoidal saponins found in swingle, the fruit of *Siraitia grosvenorii*, which have recently been widely used throughout the world as natural food sweeteners. Among this class of compounds, mogroside III E (MG III E) exhibits the most intense sweetness, and it was also found to effectively regulate blood glucose levels. However, the relative abundance of naturally occurring MG III E is low compared to other mogrosides. Therefore, the purpose of this study was to enrich MG III E through biotransformation of fruit extracts and to develop a reliable method for its purification. We used HPLC coupled with mass spectrometry and nuclear magnetic resonance spectroscopy for metabolite analysis and identified MG III E as a major metabolite of *Ganoderma lucidum* mycelium. This organism converts the most abundant mogroside, mogroside V, to MG III E via a deglycosylation reaction; high levels of β-glucosidase activities were also detected. In addition, we established an efficient purification method for MG III E using HP-20 macroporous resin. Optimization of the method was accomplished by kinetic model fitting, dynamic adsorption studies, and desorption experiments. The purity of MG III E was increased from 11.71% to 54.19%, with a 70%–76% recovery rate, and the scaled-up purification process allowed us to harvest 17.38 g of MG III E with 55.14% purity and a 74.71% of

* *Corresponding author*. Institute of Food Science and Technology, National Taiwan University, No. 1, Section 4, Roosevelt Road, Taipei 10617, Taiwan. Fax: +886 2 2362 084.
** *Corresponding author*. Institute of Food Science and Technology, National Taiwan University, No. 1, Section 4, Roosevelt Road, Taipei 10617, Taiwan.
E-mail addresses: loyichen@ntu.edu.tw (Y.-C. Lo), tjlu@ntu.edu.tw (T.-J. Lu).
[1] These authors contribute equally to this work.
https://doi.org/10.1016/j.jfda.2019.05.001
1021-9498/Copyright © 2019, Food and Drug Administration, Taiwan. Published by Elsevier Taiwan LLC. This is an open access article under the CC BY-NC-ND license (http://creativecommons.org/licenses/by-nc-nd/4.0/).

recovery rate. Therefore, our low cost, time-saving, easy to scale-up procedure for isolating MG III E could be applicable in industrial processes.

Copyright © 2019, Food and Drug Administration, Taiwan. Published by Elsevier Taiwan LLC. This is an open access article under the CC BY-NC-ND license (http://creativecommons.org/licenses/by-nc-nd/4.0/).

1. Introduction

Triterpenoids are responsible for various biological activities in several traditional Chinese herbal medicines [1]. These molecules contain both aglyone and sugar moieties, and their biological actions are determined by the type of aglycone as well as the number and arrangement of sugars in the attached side chains [1,2]. For example, mogrosides, a group of triterpenoids produced by *Siraitia grosvenorii* (Lo-Han-Kuo, LHK), exemplify how sugar moiety differences affect sweetness. The relative sweetness of mogroside VI (MG VI), mogroside V (MG V), 11-oxo-mogroside V (11-oxo-MGV), mogroside IV(MG IV), siamenoside I (S–I) and mogroside III (MG III) were measured to be 125, 378, 68, 300, 465 and 195 times sweeter than sucrose, respectively [2–4]. However, mogroside II (MG II) and mogroside I (MG I) are tasteless [2,3]. In addition to the flavor of the molecules, other biochemical activities are also influenced by the different sugar moieties. For example, the maltase inhibitory activity (IC_{50}) of MG V, MG IV, S–I, and MG III were 14, 12, 10, and 1.6 mM, respectively, while the aglycone mogrol (MG) did not inhibit the enzyme [5]. Moreover, Mogroside I E (MG I E) was shown to inhibit human promyelocytic leukemia cell (HL-60) growth, whereas MG V, MG III, mogroside II E (MG II E), mogroside I A_1 (MG I A_1), and MG did not prevent cancer cell growth [6]. Although there is no apparent consistency among mogrosides in terms of specific biological activities, the number of glucose and glycosidic linkage patterns can explain performance in sweetness, maltase inhibition, and anticancer activities.

Recently, several studies have found that the main triterpene glycosides in herbal medicines are deglycosylated by human intestinal bacteria to enrich minor components with good anticancer activity and low side effects after oral administration [7–9]. As a result, several researchers have studied the production of minor components through acid hydrolysis, enzymatic conversion, and intestinal bacteria transformation [10–12]. These studies have enabled workers to obtain suitable amounts of compounds for further investigations into their biological activities [7,13]. It has become apparent that compared to acid or alkaline hydrolysis, enzymatic reactions are often the most reliable methods to obtain specifically modified glycosides of triterpenoids. MG V is the 3-*O*-(β-D-glucopyranosyl (1 → 6)-β-D-glucopyranoside)-24-*O*(β-D-glucopyranosyl (1 → 2))-(β-D-glucopyranosyl (1 → 6)-β-D-glucopyranoside) form of MG [4,14] and was found to be the major triterpene glycoside in LHK fruits [15,16]. MG V can be converted to MG III and MG II E by cellulase or mogroside IV E (MG IV E) [17], while mogroside III E (MG III E), MG II E, mogroside IE_1 (MG I E_1) and 11-oxo-mogroside I E_1 (11-oxo-MG I E_1) can be produced by maltase treatment [14,18]. However, there is limited information on the biotransformation of naturally occurring mogrosides, which in some circumstances may be more cost-effective than enzymatic hydrolysis [19,20]. For example, MG III was transformed into MG II A_1 and MG with crude preparations of human intestinal bacteria enzymes [21], and MG V can be transformed into MG III E by yeast [22]. Therefore, the discovery of additional organisms that can efficiently biotransformation mogrosides would be invaluable for production of specific forms of mogrosides. *Ganoderma lucidum*, a group of fungi, produces several extracellular enzymes, among which β-glucosidase shows higher activity than cellulase, avicelase, pectinase, xylanase, protease, amylase, and ligninase [23]. Thus, *G. lucidum* mycelia was used to establish an efficient isoflavone glycoside bioconverting system for aglycone production [24]. Based on this previous successful application, *G. lucidum* is likely to be useful as a tool to structurally modify other mogrosides as well.

Macroporous adsorption resin (MAR) has been used to separate a variety of natural compounds, such as saponins, polyphenols and alkaloids, and is considered to be a valuable industrial purification material due to its low-cost, high-efficiency, simplicity of scale-up and ease of recycling. The main principle underlying separations by MARs is polarity preference between compounds and adsorbents, but purifications are also influenced strongly by pore diameter and surface area of adsorbents [25,26]. A mid-polar MAR called HZ 806 was previously used to purify MG V from LHK fruit, increasing the purity of MG V from 0.5% to 10.7% [26]. Here, we aimed to establish methods for biotransformation of mogroside extracts and purification of MG III E from the fermented extracts using Diaion® HP-20 (HP-20) resin. Loading and elution conditions for the HP-20 resin column were optimized, and the purification process was scaled-up 10-times to purify several grams of MG III E from a single batch.

2. Materials and methods

2.1. Strain and pre-culture preparation

G. lucidum (BCRC 37066) was purchased from the Bioresource Collection and Research Center (BCRC), Food Industry Research and Development Institute (Hsinchu, Taiwan). The mycelium of *G. lucidum* was activated with malt extract agar (Blakeslee's Formula), which is composed of 20 g of malt extract (Difco, MD, USA), 20 g of glucose (Sigma, St. Louis, MO, USA), 1.0 g of peptone (Sigma), 20 g of agar (Difco) per liter of distilled water, in a Petri dish at 25 °C for 5–7 days. *G. lucidum* was initially grown on potato dextrose broth at 25 °C, and the mycelium were harvested after 5–7 days of cultivation.

Twenty mycelial agar discs (10 mm in diameter) obtained using a sterilized cork borer were transferred to a flask containing 200 mL malt extract medium. Flasks were then incubated in an orbital shaker at 150 rpm, 25 °C for 7 days. After 7 days of incubation, the activated mycelia served as inoculums or propagules for the MG V bioconversion experiments.

2.2. Biotransformation

The raw material used for preparation of LHK water-extract solution was the dried fruit purchased from a Chinese herb store in Taipei, Taiwan. The dried fruits were crushed and ground into powder, after which the powder was dissolved in water and boiled for 10 min. Insoluble materials from the LHK powder were removed by filtration. The media designated 1% LHK and 2% LHK were LHK water-extract solutions with 1% and 2% LHK powder, respectively. Other designated media, 1% LHK + M and 2% LHK + M, were formulated by the addition of malt extract powder into 1% and 2% of LHK water-extract solutions, as appropriate. Malt extract-containing medium was used as a control. *G. lucidum* mycelium was used for mogroside bioconversion. Specifically, 5% (v/v) homogenized propagules in malt extract medium was used to inoculate the above media. Each culturing condition was comprised of triplicate samples, and the mogroside composition at 0, 3, 6, 9, 12, 15, 18 and 21 days of cultivation was monitored.

2.3. Determination of pellet size (cm) and dry weight (g)

The diameter of the mycelia was monitored using a vernier caliper to evaluate the growth of *G. lucidum*. Specifically, 50 mL samples of culture medium containing mycelia were removed from the flask and transferred onto a filter (Whatman No. 54, 20–25 μm, Maidstone Kent, England). The filter was then placed onto a Buchner funnel to separate the mycelia from media by vacuum. Before measurements were made, 150 mL of distilled water was applied with a dropper to gently remove the media absorbed on mycelia; this step improved the accuracy of the measurement. After measuring the diameter, the mycelia collected on the filter was freeze-dried, and the dry weight of mycelia was determined. The freeze-dried mycelia were then ground into mycelial powder to determine the intracellular β-glucosidase activity.

2.4. β-glucosidase activity

One unit of β-glucosidase activity was defined as the amount of enzyme that liberated 1 μmol of *p*-nitrophenol per min at 30 °C. The β-glucosidase activity of the mycelia was determined by the conversion of *p*-Nitrophenyl-β-D-glucopyranoside (*p*NPG; Sigma–Aldrich, St. Louis, MO, USA) to *p*-nitrophenol (*p*NP), which can be analyzed colorimetrically at 420 nm (Helios Omega spectrophotometer, Thermo Fisher Scientific Inc., Waltham, USA). A standard curve of *p*NP, with concentrations ranging from 0 to 0.4 mM, was established by diluting 10 mM *p*NP stock solution (Merck KGaA, Darmstadt, Germany) with sodium acetate buffer. The curve was then used to evaluate the amount of *p*NP liberated from *p*NPG by β-glucosidase in the test samples, which consisted of the mycelial powders collected from different fermentation stages described above. Briefly, 100 mg of mycelial powder was mixed with 3 mL 0.1 M phosphate-citrate buffer (pH 5.0) for 1 min, followed by centrifugation (15,000 rpm, 4 °C, 20 min) to collect the supernatants. Aliquots of enzyme solution (0.5 mL) were added to 2 mL *p*NPG (1 mM), which was prepared by dissolving the *p*NPG in 0.1 M of phosphate-citrate buffer (pH 5.0) and preheating at 30 °C for 5 min. After the addition of enzyme solution, the reaction mixture was incubated at 30 °C for 30 min, and the reaction was terminated by adding 2.5 mL 0.5 M sodium carbonate (ACS grade, Mallinckrodt Baker, Phillipsburg, NJ, USA). To evaluate the amount of *p*NP released, the OD_{420nm} of each sample was measured immediately using a spectrophotometer.

2.5. HPLC-ESI-MS analysis

Mogrosides were identified by negative ion electrospray using a Thermo Finnigan model LXQ Linear Ion Trap Mass Spectrometer (San Jose, CA, USA) equipped with an HPLC system. The HPLC included a photodiode array detector (Surveyor PDA plus), pump (Surveyor MS Pump Plus) and autosampler (Surveyor Autosampler plus), respectively. The YMC Hydrosphere C18 analytical column (2.0 × 150 mm, 5 μm; YMC, Kyoto, Japan) was maintained at room temperature and used with a flow-rate of 0.2 mL/min. The mobile phase consisted of (A) water (Milli-Q; Millipore, Billerica, MA) and (B) methanol (HPLC grade; Mallinckrodt Baker, Philipsburg, NJ, USA), both of which contained 0.01% formic acid (98–100% analytical grade; RdH, Seelze, Germany). Gradients were programmed as follows: 45% B at 0–5 min, 45–75% B at 5–45 min, 75–100% B at 45–50 min, constant 100% B at 50–55 min, 100-45% B at 55–60 min, and constant 45% B at 60–70 min. The sample (25 μL) was injected by the autosampler and photodiode array detector was used at 200–600 nm. The ESI parameters were set as follows: spray voltage was −6.0 kV, the capillary temperature was 400 °C, sheath gas was 21 arb, auxiliary gas was 10 arb, sweep gas was 5 arb, collision energy was 20%, isolation width was 2.0 Da, and scan range was 50–2000 *m/z*. Xcalibur 2.0.7 software was used for data analysis (San Jose, CA, USA). A standard curve (0–3.89 × 10^{-2} nmole) was established using 7.78 × 10^{-2} nmol MG V (CHEMOS GmbH Co, Regenstauf, Germany) in methanol.

2.6. ^{1}H and ^{13}C NMR spectroscopy

^{1}H and ^{13}C NMR spectra and ^{1}H-^{1}H COSY, NOSEY, HSQC, and HMBC were recorded using a 500 MHz or 800 MHz NMR (Bruker AVIII, Fallanden, Switzerland) spectrometer in C_5D_5N.

2.7. Static adsorption isotherm and adsorption kinetics

The equilibrium adsorption isotherm was obtained by mixing 10 mL of water-adjusted samples, containing 7.50, 18.75, 37.5, 52.50, 63.75 and 75.00 mg/mL of dried fermented powders, with 1 g (dry weight) of HP-20 resin into separate test tubes. The fermented powders were the lyophilized culture filtrate of fermented LHK broth. The LHK broth was prepared by dissolving 1% LHK powder purchased from Changsha Huir Biological-tech Co. Ltd, a commercially available powder containing 25% MG V. Culture conditions were optimized to

obtain the highest MG III E bioconversion rate. The test tubes were then sealed and shaken at 150 rpm for 6 h at 25 °C. The remaining unadsorbed MG III E was collected from the supernatant and purified on a C18-solid phase extraction (SPE) column before determination of the equilibrium MG III E concentration by HPLC-MS analysis. MG III E standard compound for analysis and identification was collected from previous study [22]. The equilibrium adsorption capacity was calculated according to the equation (1):

$$q_e = (C_0 - C_e)V_i / M \quad (1)$$

where q_e (mg/g) is the equilibrium adsorption capacity (indicating the amount of MG III E adsorbed onto the adsorbent at equilibrium), C_0, and C_e (mg/mL) are the initial and equilibrium MG III E concentrations, respectively. V_i (mL) is the volume of the adsorption solution, M (g) is the dry weight of the resin.

Adsorption kinetics were measured by first mixing 1 g (dry weight) of HP-20 resin and 10 mL of a water-adjusted sample containing 37.5 mg/mL of dried fermented powder in a test tube. The mixture was vigorously shaken at 150 rpm and sampled at different time points for analysis of MG III E content. The adsorption capacity was calculated according to the equation (2):

$$q_t = (C_0 - C_t)V_i / M \quad (2)$$

where q_t (mg/g resin) indicates the amount of MG III E adsorption at time t, and C_t (mg/mL) is the adsorption capacity and concentration of MG III E at time t.

2.8. Dynamic adsorption and desorption tests

The dynamic adsorption and desorption tests were carried out in a glass column (25 × 250 mm), which was wet-packed with 15 g (dry weight) HP-20 resin with a 24.3 mL bed volume (BV: the total volume of HP-20 in the column). Water-adjusted sample containing 37.5 mg/mL dried fermented powders, pH 10, was loaded into the glass column at rates of 2, 3, and 4 BV/h. The liquid flowing from the column outlet was collected in 1.5 BV fractions and used for MG III E content analysis to determine the dynamic adsorption characteristics of MG III E.

After loading at least 12 BV sample solution (37.5 mg/mL) to reach a breakthrough point, the column was eluted with a gradient of aqueous ethanol from 0% to 45%. The eluent was collected in 5 BV fractions for a total of 45 BV. The eluate fractions were analyzed by HPLC-MS to determine desorption behavior. The desorption ratio of one elution fraction was calculated by equation (3), whereas the cumulative desorption ratio was calculated according to equation (4),

$$D_x = (C_{dx}V_{dx}/(C_{in} - C_{out})V_a)100 \quad (3)$$

$$D_c = \sum Dx \quad (4)$$

where C_{in} (mg/mL) is the concentration of target compound in the loading solution, C_{out} (mg/mL) is the concentration of target compound at the outlet, V_a (mL) is the volume of loading solution, C_{ds} (mg/mL) is the concentration of target compound in x elution fraction, and V_{dx} (mL) is the volume of elution fraction x.

2.9. Scaled-up purification

A scaled-up purification of MG III E was carried out in a glass column (25 × 250 mm) wet packed with 150 g (dry weight) HP-20 resin with a BV of 243.2 mL. Twelve bed volumes of fermented product aqueous solution (37.5% mg/mL) were fed through the HP-20 resin column, which was then washed with 5 BV of ultrapure water and 3 BV 10% ethanol to remove impurities. The column was then eluted with 9 BV 40% ethanol to collect MG III E. Ethanol was removed from the collected eluents on a rotary evaporator and then the eluents were introduced to a freeze-dryer after freezing for removing the remaining water. The purity of MG III E in 40% ethanol was calculated by equation (5), and the recovery rate of MG III E during the process was calculated as equation (6).

$$P_x = (W_{xIII\ E}/W_x)100\% \quad (5)$$

$$R_x = (W_xP_x/W_aP_a)100\% \quad (6)$$

W_a (mg) is the weight of the crude sample, P_a is the purity of the target compound in the crude sample. P_x is the purity, $W_{x\ III\ E}$ (mg) is the weight of target compound inside elution fraction, W_x (mg) is the total weight of the elution fraction.

3. Results and discussion

3.1. Effect of mogrosides on mycelium of G. lucidum and metabolite analysis

To evaluate the growth of mycelia in LHK water extract, we examined the dried mass and pellet size of mycelia in malt-extract control medium, malt-extract medium containing 1% and 2% LHK water-extract solution, and LHK water-extract solution alone. The results are presented as dried mass (Fig. 1a) and pellet size (Fig. 1b) of mycelia. Two percent LHK water-extract supplemented with a malt-extract medium (2% LHK + M) was the best medium, as the two components synergistically promoted mycelium growth compared to LHK and malt-extract alone.

In order to monitor mogroside conversion, the concentrations of mogroside metabolites were measured by HPLC-ESI-tandem MS. MG V was found to be the major triterpene glycoside in the LHK water-extract solution. The ESI/MS^n spectra of mogrosides displayed predominant molecular ions $[M-H]^-$, with sequential glucose losses (−162) in the collision-induced dissociation mode (Supplementary Material Table S1). In addition, an [aglycone-H]$^-$ ion at *m/z* 475.5, corresponding to the mogroside aglycone moiety was observed for all mogrosides. This fragmentation pattern provided structural information to identify the individual compounds by molecular weight at each retention time.

The deglycosylation of MG V by *G. lucidum* mycelium in the broth of LHK water-extract solution with or without the addition of malt-extract medium could be distinguished by the presence of peak 4 and peak 5 in the ESI/MS^n spectra (Fig. 1c–h). Peak 4 was determined to be $C_{48}H_{82}O_{19}$ (negative ion mode; $[M-H]^-$, *m/z* 961.5). In fact, the ^{13}C NMR spectrum of the peak 4 aglycone moiety was very similar to mogrol [27,28],

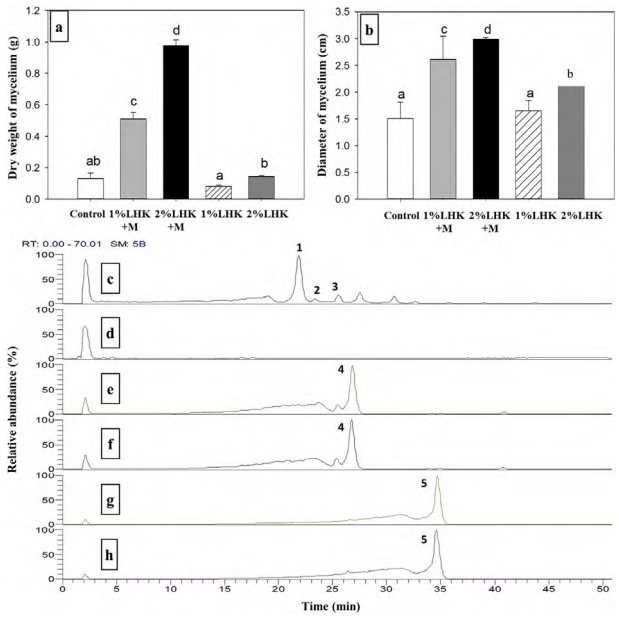


Fig. 1 – Effects of carbon supplementation on mycelium growth and metabolites during mogroside conversion. (a) The dry mass and (b) the size of mycelium of *G. lucidum* after 21-day cultivation in malt extract-containing medium (carbon source control, represented as M), malt extract-containing medium with 1% or 2% LHK water-extract solution (1% LHK + M or 2% LHK + M) and 1% or 2% LHK water-extract solution (1% LHK or 2% LHK). Different letters indicate significant differences, determined by ANOVA with Tukey's HSD post hoc test ($p < 0.05$). Metabolite analyses using LC-MS are shown as chromatograms with signals of base peak. (c) Mogrosides from LHK water-extract solution and *G. lucidum* fermentation broth of (d) malt extract (control), (e) 1% LHK + M, (f) 2% LHK + M, (g) 1% LHK, (h) 2% LHK cultivated for 21 days. 1, mogroside V (MG V); 2, siamenoside I (S–I); 3, mogroside IV (MG IV); 4, mogroside III E (MG III E); 5, mogroside II A (MG II A).

which had three β-anomeric proton signals at 5.36 (1H, d, $J = 7.8$ Hz), 5.11 (1H, d, $J = 7.8$ Hz), and 4.91 (1H, d, $J = 7.9$ Hz) in the ^{1}H NMR spectrum. In addition, there were three anomeric carbon signals at 102.2, 106.8 and 107.8 ppm in the ^{13}C NMR spectrum (Supplementary Material Table S2). Overall, peak 4 had the same structural characteristics as reported by Matsumoto et al. (1990) for MG III E, indicating the compound in peak 4 was indeed MG III E [29].

Meanwhile, peak 5 exhibited $[M-H]^-$ at *m/z* 799.5, MS^2 *m/z* 637.5 $[799.5-C_6H_{10}O_5]^-$, MS^3 *m/z* 475.5 $[637.5-C_6H_{10}O_5]^-$ in the ESI/MS^n, corresponding to a molecular formula of $C_{42}H_{72}O_{14}$. Additionally, peak 5 showed two β-anomeric proton signals at 5.38 (1H, d, $J = 7.8$ Hz) and 5.11 (1H, d, $J = 7.8$ Hz) in the ^{1}H NMR spectrum and anomeric carbon signals at 102.2 and 106.8 ppm in the ^{13}C NMR spectrum. In a comparison with the spectroscopic data for MG III E, peak5 was missing a β-D-glucopyranoside moiety at C-3 of MG III E. Hence, the structure of peak 5 was determined to be the 24-O-β-D-glucopyranosyl (1 → 2)-β-D-glucopyranoside of MG (MG II A). According to our results, the major metabolite of MG V was the triterpene triglucoside, MG III E. However, the mycelia of *G. lucidum* were able to further utilize one glucosyl residue on MG III E and convert it to the triterpene diglycoside under carbon source-restricted conditions.

In order to better understand the relationship between mogrosides biotransformation patterns and incubation time, the amount of each mogroside (nmole) in the fermentation broth was investigated by HPLC-tandem-MS^n (Fig. 2a–d). MG V was predominantly present in the LHK water-extract solution at the start of the biotransformation process. We noticed that although the total mogroside content was not decreased, MG V was converted to deglucosyl forms in four experimental conditions (1%LHK + M, 2%LHK + M, 1% LHK, and 2% LHK). The amount of MG V decreased with increased fermentation time, while MG III E and other mogrosides, such as MG IV, S–I, and MG II A, gradually increased. Therefore, our results show that LHK water-extract solution is not only capable of sustaining the growth of mycelium, but the MG V within the solution is converted to MG III E and MG II A (Fig. 2e). However, the mechanism of mogroside conversion was not known. In addition, after initially finding that the cell-free enzyme solution worked without co-enzyme, we immediately thought of extracellular and intracellular enzyme purification. However, even after the enzymes from two different sources were concentrated and used for mogroside conversion, we still could not obtain a conversion rate as high as the cell-based method. In addition, there is no commercially available enzyme for us to test as positive control and no MG II A was found when the extracellular enzyme extracts were used. Therefore, in order to acquire consistent results for each mogroside conversion batch, we chose the cell-based method for mogroside bioconversion. However, before conducting further studies, we first decided to analyze the β-glucosidase activity of the mycelium during the biotransformation process, as this enzyme is often responsible for glycosidic bond cleavages in glycosides [24].

3.2. β-glucosidase assays of the mycelia

The β-glucosidase activity in the mycelia of *G. lucidum* reflects the glycoside-metabolizing activity of the organism, and our measurements of this activity are shown in Fig. 3a. The β-glucosidase activities of mycelia cultivated in the media containing only 1% or 2% LHK were significantly higher and appeared to peak around day 3 compared to the activities of mycelia obtained from LHK media supplemented with malt extract. Although these results might explain the appearance of MG II A, which represents the loss of one more glucose from MG III E (caused by higher β-glucosidase activity), we still cannot exclude the possibility that induction of protein expression for other forms of β-glucosidases may be responsible for the additional glucose cleavage under carbon-limited cultivation conditions [30]. For example, cellulose contributed to MG II A production, as reported by Murata in 2010 [17]. In addition, previous studies using yeast mutants to convert MG V into MG III E during fermentation had concluded that the mutation of *KRE6* in yeast could increase the secretion of extracellular β-glucosidases and accelerate the conversion of MG III E [22,31]. In fact, a previous study confirms that a gene in *G. lucidum* called *GLP2* had a similar function to yeast *KRE6*

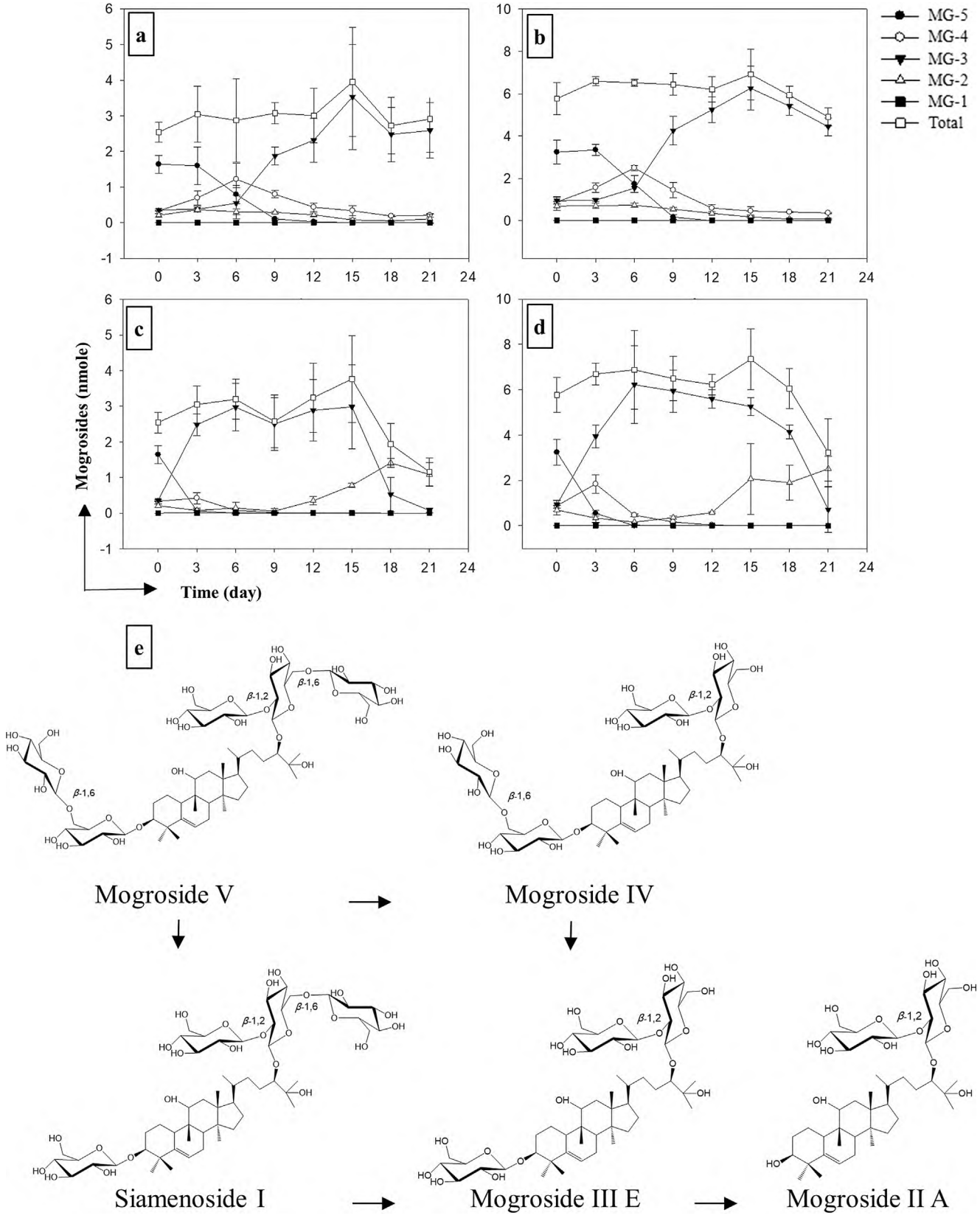


Fig. 2 – Change of mogroside content during the culture of *G. lucidum* in (a) 1% LHK + M (malt-extract medium represented as M), (b) 2% LHK + M, (c) 1% LHK, and (d) 2% LHK. (e) Biotransformation pathways of MG V during the conversion process are shown.

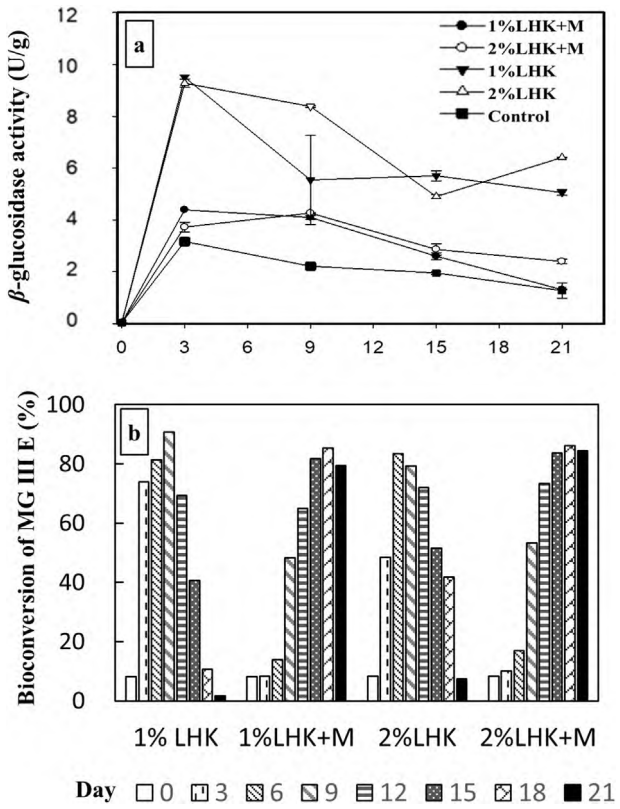


Fig. 3 – Effect of medium composition on the (a) β-glucosidase activity (U/g) and (b) MG III E bioconversion rate of *G. lucidum*. The bioconversion rates of MG III E are calculated as nmole of MG III E formed per nmole of total MG.

[32], indicating that deletion of *GLP2* in *G. lucidum* might further increase the β-glucosidase activity and accelerate the biotransformation process. Fig. 3b shows the bioconversion rates of MG III E in each medium at different time points, as calculated from Fig. 2. Media containing only LHK yielded better bioconversion rates at early fermentation time-points compared to LHK media containing malt extract. However, the rate gradually decreased after 9 days of fermentation. In order to obtain starting materials with high levels of MG III E for purification, we decided to collect the supernatants of 2% LHK media after 9 days of fermentation from the culture. These supernatants were then processed into powder by lyophilization.

3.3. *Adsorption and desorption behavior of MG III E on the HP-20 resin*

Our preliminary studies showed that mogrosides could be purified by non-polar or weak-polar macroporous adsorption resins. Therefore, we first decided to test whether a non-polar HP-20 resin is suitable for the separation of MG III E from the media containing LHK water extract after fermentation. We plotted the static adsorption isotherm of MG III E according to equation (1), for which the longitudinal axis is q_e (equilibrium adsorption capacity) and the horizontal axis is C_e (equilibrium MG III E concentration). The results showed that q_e will change along with the initial loading concentration of MG III E. In other words, the higher the C_e, the larger the q_e of MG III E (Fig. S1). In addition, the established static adsorption isotherm shown in Fig. S1 enabled us to describe the adsorption behavior of MG III E on HP-20 through model fitting. Fitting of models, including the Langmuir and Freundlich models can respectively describe a monolayer adsorption, and both monolayer and multilayer adsorption behaviors [33]. Through performing these fittings, we found that the correlation coefficient of the Freundlich model was higher than Langmuir model (Table 1), indicating that the MG III E adsorption behavior is a mix of monolayer and multilayer adsorption. In addition, if the value of 1/n falls between 0.1

Table 1 – Adsorption isotherm models of MG III E on HP-20 resin at 25°C.

Isotherm model	Equation	Parameters
Langmuir	$q_e = \frac{940.3C_e}{1+10.77C_e}$	$k_L = 10.77$[a] $q_m = 87.31$[c] $R^2 = 0.9312$[e]
Freundlich	$q_e = 70.18\ C_e^{0.2765}$	$k_F = 70.18$[b] $1/n = 0.2765$[d] $R^2 = 0.9845$[e]

Data are presented as the average of two experiments. The models were fitted by SigmaPlot 12.5 software, and all parameters were output.
[a] k_L is the Langmuir adsorption equilibrium constant.
[b] k_F is the Freundlich adsorption equilibrium constant.
[c] q_m (mg/g resin) is the theoretical maximum adsorption capacity.
[d] 1/n is an empirical constant related to the magnitude of the adsorption driving force.
[e] R^2 is the correlation coefficient of the equation.

Table 2 – Adsorption kinetic models for MG III E on the HP-20 resin.

Kinetic model	Equation	Parameters
Pseudo-first-order	$lg(44.27-q_t) = lg44.27-\frac{0.0653}{2.303}t$	$k_1 = 0.0653$[a] $q_e = 44.27$[d] $R^2 = 0.9818$[f]
Pseudo-second-order	$\frac{t}{q_t} = \frac{1}{48.35}t + \frac{1}{0.0020\times 48.35^2}$	$k_2 = 0.0020$[b] $q_e = 48.35$[d] $R^2 = 0.9777$[f]
Intraparticle diffusion	$q_t = 1.5889t^{\frac{1}{2}} + 24.73$	$k_{id} = 1.5889$[c] $C = 24.73$[e] $R^2 = 0.7076$[f]

Data are presented as the average of two experiments. The models were fitted by SigmaPlot 12.5 software, and all parameters were output.
[a] k_1 (min^{-1}).
[b] k_2 (g/mg*min).
[c] k_{id} (g/mg $min^{-1/2}$) are the rate constants of pseudo-first-order, pseudo-second-order and intraparticle diffusion, respectively.
[d] q_e (mg/g resin) is the adsorption capacity when reaching adsorption equilibrium.
[e] C (mg/g) is an empirical constant representing boundary layer thickness.
[f] R^2 is the correlation coefficient of the equation.

and 0.5, the target compound is considered easy to adsorb. If 1/n is higher than 1, the target compound is considered hard to adsorb [34,35]. Our results showed that 1/n in the Langmuir model was 0.27, indicating that MG III E was easy to adsorb onto the HP-20 resin. Moreover, we also discovered that 37.5 mg/mL of MG III E was the lowest initial concentration to produce a relatively high q_e (60 mg/g), when compared to initial MG III E concentrations of 52.50, 63.75, 75.00 mg/mL (Fig. S1). Therefore, we used 37.5 mg/mL MG III E solution as the optimal sample loading concentration in further experiments.

After finding that HP-20 is a suitable material for MG III E adsorption, we then shifted our attention to understanding the adsorption rate of MG III E. This goal was accomplished by studying the adsorption kinetics of MG III E in HP-20 by the adsorption rate curve shown in equation (2). The adsorption rate curve could also be well fitted with models describing the adsorption mechanism [36]. Although the results of the model fitting shown in Table 2 have large coefficients for both pseudo-first-order and pseudo-second-order models, the theoretical value of q_e, 44.27 mg/g in the pseudo-first-order model is close to the actual MG III E concentration of 45.89 mg/g at 240 min (Fig. S2). Therefore, the pseudo-first-order model performed better at predicting the adsorption rate of MG III E on HP-20.

3.4. *Purification of MG III E and its scale-up*

3.4.1. *Dynamic adsorption test*

In dynamic adsorption, the loading rate and loading volume of the sample are both important factors to consider for scale-up purification in order to save time and avoid sample loss. For example, a high loading rate may save time, but it will lead to sample loss due to a shortage of sample–resin interaction time. Additionally, a large loading volume may also result in leakage of the sample due to overloading. Generally, in order to optimize loading rate and volume, the amount of sample leakage at the outlet of the column should be between 5% and 10% of the initial sample loading concentration (37.5 mg/mL). Our results showed that when the total sample loading volume was lower than 12 BV under different loading rates (2, 3 and 4 BV/h), the proximal breakthrough point was always less than 5% (Fig. 4a), and 95% of loaded samples were successfully adsorbed onto the HP-20 resin. Therefore, a loading rate of 4 BV/h was selected to maximize time efficiency; this value was also chosen as the elution rate.

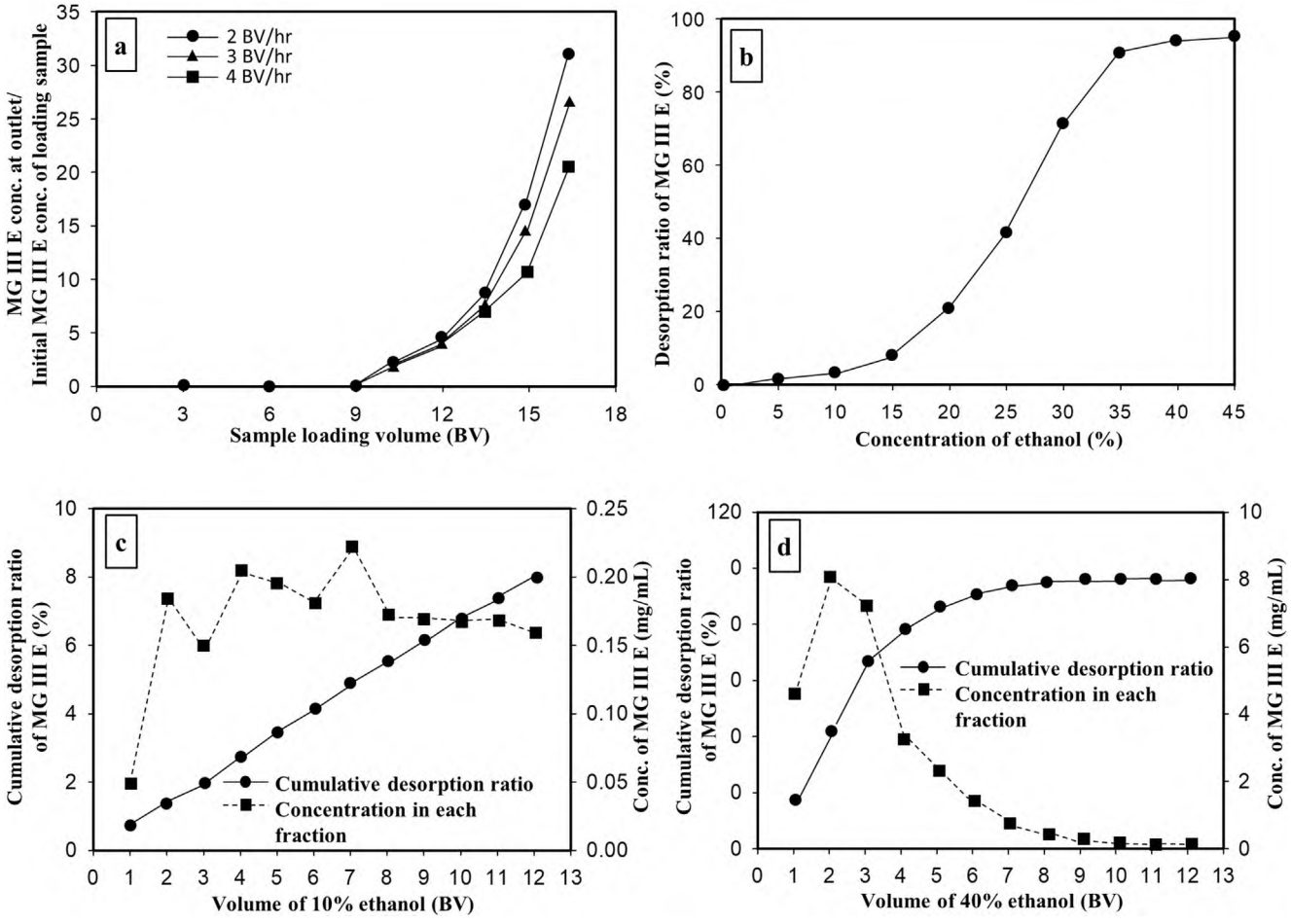


Fig. 4 – (a) Dynamic breakthrough curves of MG III E on HP-20 resin at different loading rates. (b) Dynamic desorption curve of MG III E from the HP-20 resin using different concentrations of aqueous ethanol. (c) Dynamic desorption curves of MG III E from the HP-20 resin using 10% ethanol for impurity removal and (d) 40% ethanol for elution. Data are presented as the average of two experiments.

Table 3 – MG III E purification by HP-20 resin column.

	HP-20 scale (g)	Loading Crude MG III E (g)	Product Weight (g)	MG III E purity (%)	MG III E recovery (%)
Crude MG III E[1]	–	–	–	11.71±0.26	–
MG III E –a[2]	15	10.94	1.71±0.01	54.19±1.36	72.23±1.64
MG III E –b[3]	150	109.44	17.38±0.44	55.14±2.44	74.71±1.41

[1]Fermentation sample; [2,3]purification products from HP-20 resin columns at different scales. Data are presented as the mean ± SD of three experiments, and statistical analysis was performed using Student's *t*-test.

3.4.2. *Dynamic desorption curves*

In order to improve the cost-effectiveness of desorption, a dynamic desorption test with gradient aqueous ethanol was conducted to optimize the concentration of ethanol used to elute MG III E from the column. Fig. 4b illustrates the total desorption ratio of MG III E from HP-20 resin in different ethanol concentrations, ranging from 0% to 45% (v/v). The cumulative desorption ratio of MG III E calculated from equation (3) rose slowly from 0% to 15% and increased sharply from 20% to 35% ethanol. Notably, 3.65% of MG III E was eluted at 10% ethanol, while 94.17% MG III E was eluted at 40% ethanol. When we looked back at the results from Fig. 4b (the desorption ratio of MG III E under different ethanol concentration), we found that the major loss of target compounds occurred during the 10% ethanol wash to remove impurities. However, there was always a trade-off between purity and the recovery percentage. For example, if we use 5% of ethanol instead of 10% of ethanol to remove impurities, we could obtain a high recovery rate, but lower purity compound would also be obtained. Therefore, an ethanol concentration of 10% was selected to remove impurities, and an ethanol concentration of 40% was used for eluting MG III E from the resin.

The column was first loaded with sample to the sample breakthrough point (loading 12 BV sample at 37.5 mg/mL) prior to performing the dynamic desorption test. During the desorption test, the column was washed with 5 BV water, followed by removal of impurities with 3 BV of 10% ethanol. This washing protocol was used because less than 2% of the MG III E was lost when keeping the washing volume below 3 BV, according to equation (4) (Fig. 4c, solid line). In addition, when eluted with 40% ethanol, the cumulative desorption ratio of MG III E rose rapidly to 95.60% below 9 BV, which implied nearly all the MG III E was collected (Fig. 4d).

3.4.3. *Purification of MG IIIE and its scale-up*

Table 3 shows the purification results of MG III E for two scales, including columns containing 15 g and 150 g of HP-20 resin. The purity of MG III E was increased significantly at both scales, as calculated according to equation (5). In the large column, the purity of MG III E increased from 11.71% to 55.14%, while also maintaining a 74.71% recovery rate, according to equation (6). The separation technique described here was suitable to harvest 17.38 g of MG III E with 55.14% (w/w) purity and could easily be applied to commercial production of high-quality MG III E from biotransformed mixtures. Although we can increase the purity of the target compound by increasing the volume of the purification column by allowing more absorptive interactions between MG III E and HP-20 resin and increase the theoretical plate numbers that contribute to better separation, the limited funding and space of this study only allow us to obtain 55% MG III E purity. Currently, there are several commercially available mogroside powders available. All of which are MG V with purity ranging from 25% to 80%. Therefore 55% MG III E purity should be acceptable for use in the food industry as a natural sweetener. However, the amount of MG II A produced in our method was quite low in terms of industrial use, mainly because the conversion rate of MG II A was only about 25%

4. Conclusion

In this study, we showed the effect of medium on *G. lucidum* mycelium-mediated mogroside conversion. We discovered that a limited carbon source could drive the *G. lucidum* mycelium to shift its main metabolite of mogrosides from MG III E to MG II A. Therefore, this is the first report to show that *G. lucidum* is capable of specifically producing MG III E and MG II A, depending on the media composition, and the MG III E β-(1,2) linkage of glucosyl is more resistant to hydrolysis by β-glucosidase. In addition, our analysis of triterpenoids and metabolites was highly accurate, using HPLC coupled with tandem mass spectrometry (MS^n). Furthermore, we found that MG III E could be purified from the fermentation product using HP-20 resin under alkaline conditions. The scaled-up purification process (150 g of HP-20 resin) allowed us to collect 17.38 g MG III E with a 74.71% recovery rate and 55.14% purity.

Conflicts of interest

All authors declare that they have no conflict of interest.

Acknowledgments

This research was supported by the by the National Science Council of Taiwan ROC (NSC 102-2313-B-002-057).

Appendix A. Supplementary data

Supplementary data to this article can be found online at https://doi.org/10.1016/j.jfda.2019.05.001.

REFERENCES

[1] Connolly JD, Hill RA. Triterpenoids. Nat Prod Rep 2005;22:230–48.
[2] Kalinowska M, Zimowski J, Pączkowski C, Wojciechowski AZ. The formation of sugar chains in triterpenoid saponins and glycoalkaloids. Phytochem Rev 2005;4:237–57.
[3] Murata Y, Yoshikawa S, Suzuki YA, Sugiura M, Inui H, Nakano Y. Sweetness characteristics of the triterpene glycosides in *Siraitia grosvenori*. J Jpn Soc Food Sci 2006;53:527–33 [In Japanese, English abstract].
[4] Takemoto T, Arihara S, Nakajima T, Okuhira M. Studies on the constituents of fructus *Momordicae*. I. On the sweet principle. Yakugaku Zasshi 1983;103:1151–4 [In Japanese, English abstract].
[5] Suzuki YA, Murata Y, Inui H, Sugiura M, Nakano Y. Triterpene glycosides of *Siraitia grosvenori* inhibit rat intestinal maltase and suppress the rise in blood glucose level after a single oral administration of maltose in rats. J Agric Food Chem 2005;53:2941–6.
[6] Mizushina Y, Akihisa T, Hayakawa Y, Takeuchi T, Kuriyama I, Yonezawa Y, et al. Structural analysis of mogrol and its glycosidcs as inhibitors of animal DNA polymerase and human cancer cell growth. Lett Drug Des Discov 2006;3:253–60.
[7] Bae EA, Han MJ, Choo MK, Park SY, Kim DH. Metabolism of 20(S)- and 20(R)-ginsenoside R-g3 by human intestinal bacteria and its relation to in vitro biological activities. Biol Pharm Bull 2002;25:58–63.
[8] Hasegawa H, Lee KS, Nagaoka T, Tezuka Y, Uchiyama M, Kadota S, et al. Pharmacokinetics of ginsenoside deglycosylated by intestinal bacteria and its transformation to biologically active fatty acid esters. Biol Pharm Bull 2000;23:298–304.
[9] Ye L, Zhou CQ, Zhou W, Zhou P, Chen DF, Liu XH, et al. Biotransformation of ginsenoside Rb1 to ginsenoside Rd by highly substrate-tolerant Paecilomyces bainier 229-7. Bioresour Technol 2010;101:7872–6.
[10] Cai ZW, Qian TX, Wong RNS, Jiang ZH. Liquid chromatography-electrospray ionization mass spectrometry for metabolism and pharmacokinetic studies of ginsenoside Rg3. Anal Chim Acta 2003;492:283–93.
[11] Karikura M, Miyase T, Tanizawa H, Taniyama T, Takino Y. Studies on absorption, distribution, excretion and metabolism of ginseng saponins .6. The decomposition products of ginsenoside Rb2 in the stomach of rats. Chem Pharm Bull (Tokyo) 1991;39:400–4.
[12] Ko S, Suzuki Y, Suzuki K, Choi K, Cho B. Enzymatic preparation of minor saponins and intestinal bacterial saponin metabolites of ginseng. Part III". Marked production of ginsenosides Rd, F-2, Rg(3), and compound K by enzymatic Method. Chem Pharm Bull (Tokyo) 2007;55:1522–7.
[13] Tawab MA, Bahr U, Karas M, Wurglics M, Schubert-Zsilavecz M. Degradation of ginsenosides in humans after oral administration. Drug Metab Dispos 2003;31:1065–71.
[14] Takemoto T, Arihara S, Nakajima T, Okuhira M. Studies on the constituents of fructus *Momordicae*. II. Structure of sapogenin. Yakugaku Zasshi 1983;103:1155–66.
[15] Makapugay HC, Nanayakkara NPD, Soejarto DD, Kinghorn AD. High-performance liquid chromatographic analysis of the major sweet principle to Lo Han Kuo fruits. J Agric Food Chem 1985;33:348–50.
[16] Zhou Y, Zheng Y, Ebersole J, Huang CF. Insulin secretion stimulating effects of mogroside V and fruit extract of Luo han kuo (*Siraitia grosvenori* Swingle) fruit extract. Yao Xue Xue Bao 2009;44:1252–7 [In Chinese, English abstract].
[17] Murata Y, Ogawa T, Suzuki YA, Yoshikawa S, Inui H, Sugiura M, et al. Digestion and absorption of *Siraitia grosvenori* triterpenoids in the rat. Biosci Biotechnol Biochem 2010;74:673–6.
[18] Takemoto T, Arihara S, Nakajima T, Okuhira M. Studies on the constituents of fructus *Momordicae*. III. Structure of mogrosides. Yakugaku Zasshi 1983;103:1167–73 [In Japanese, English abstract].
[19] Kuo HP, Wang R, Huang CY, Lai JT, Lo YC, Huang ST. Characterization of an extracellular beta-glucosidase from *Dekkera bruxellensis* for resveratrol production. J Food Drug Anal 2018;26:163–71.
[20] Kuo HP, Wang R, Lin YS, Lai JT, Lo YC, Huang ST. Pilot scale repeated fed-batch fermentation processes of the wine yeast *Dekkera bruxellensis* for mass production of resveratrol from *Polygonum cuspidatum*. Bioresour Technol 2017;243:986–93.
[21] Yang XW, Zhang JY, Xu W. Biotransformation of mogroside III by human intestinal bacteria. Beijing Da Xue Xue Bao Yi Xue Ban 2007;39:657–62 [In Chinese, English abstract].
[22] Chiu CH, Wang R, Lee CC, Lo YC, Lu TJ. Biotransformation of mogrosides from *Siraitia grosvenorii* swingle by *Saccharomyces cerevisiae*. J Agric Food Chem 2013;61:7127–34.
[23] Jo W-S, Park H-N, Cho D-H, Yoo Y-B, Park S-C. Detection of extracellular enzyme activities in *Ganoderma neo-japonicum*. Mycobiology 2011;39:118–20.
[24] Miura T, Yuan L, Sun BX, Fujii H, Yoshida M, Wakame K, et al. Isoflavone aglycon produced by culture of soybean extracts with basidiomycetes and its anti-angiogenic activity. Biosci Biotechnol Biochem 2002;66:2626–31.
[25] Zhang Y, Li S, Wu X, Zhao X. Macroporous resin adsorption for purification of flavonoids in houttuynia cordata thunb. Chin J Chem Eng 2007;15:872–6.
[26] Zhang M, Yang H, Zhang H, Wang Y, Hu P. Development of a process for separation of mogroside v from *Siraitia grosvenorii* by macroporous resins. Molecules 2011;16:7288–301.
[27] Zhang JY, Yang XW. Assignments of ^{1}H and ^{13}C NMR signals of mogroside IVa. J Chin Pharm Sci 2003:196–200.
[28] Akihisa T, Hayakawa Y, Tokuda H, Banno N, Shimizu N, Suzuki T, et al. Cucurbitane glycosides from the fruits of *Siraitia grosvenorii* and their inhibitory effects on Epstein-Barr virus activation. J Nat Prod 2007;70:783–8.
[29] Matsumoto K, Kadai R, Ohtani K, TAnaka O. Minor cucurbitane-glycosides from fruits of *Siraitia grosvenori* (cucurbitaceae). Chem Pharm Bull (Tokyo) 1990;38:2030–2.
[30] Manavalan T, Manavalan A, Thangavelu KP, Heese K. Secretome analysis of *Ganoderma lucidum* cultivated in sugarcane bagasse. J Proteomics 2012;77:298–309.
[31] Wang R, Lin PY, Huang ST, Chiu CH, Lu TJ, Lo YC. Hyperproduction of beta-glucanase Exg1 promotes the biotransformation of mogrosides in *Saccharomyces cerevisiae* mutants defective in mannoprotein deposition. J Agric Food Chem 2015;63:10271–9.
[32] Shiau S-S. Molecular cloning and characterization the SKN1 gene family of *Ganoderma lucidum*. MSD thesis. Taipei: National Taiwan University; 2006.
[33] Foo KY, Hameed BH. Insights into the modeling of adsorption isotherm systems. Chem Eng J 2010;156:2–10.
[34] Fu Y, Zu Y, Li S, Sun R, Efferth T, Liu W, et al. Separation of 7-xylosyl-10-deacetyl paclitaxel and 10-deacetylbaccatin III from the remainder extracts free of paclitaxel using macroporous resins. J Chromatogr A 2008;1177:77–86.
[35] Fu Y, Zu Y, Liu W, Efferth T, Zhang N, Liu X, et al. Optimization of luteolin separation from pigeonpea [*Cajanus cajan* (L.) *Millsp.*] leaves by macroporous resins. J Chromatogr A 2006;1137:145–52.
[36] Ho YS, McKay G. Pseudo-second order model for sorption processes. Process Biochem 1999;34:451–65.